EFFECT OF ACTIVE MUSCLE FORCES ON KNEE INJURY RISKS FOR PEDESTRIAN STANDING POSTURE AT LOW SPEED IMPACTS

Chawla A, Mukherjee S, Soni A

Department of Mechanical Engineering, Indian Institute of Technology, New Delhi, INDIA

Malhotra R,

Department of Orthopaedics, All India Institute of Medical Sciences, New Delhi. INDIA

ABSTRACT

Unlike car occupants, pedestrian crashes occur in a variety of postures (like stationary, walking, running or jogging etc). Muscle contraction, required to maintain the initial posture, modifies the load at the knee joint in rapid loading conditions. This study investigates the effect of muscle active forces on lower extremity injuries for various impact locations and impact angles for a freely standing pedestrian. Three different pre-impact conditions of a freely standing pedestrian, representing a cadaver, an unaware and an aware braced pedestrian, have been simulated for each impact orientation. Stretch based reflexive action was included in the simulations for an unaware pedestrian. It is concluded that strain in knee ligaments is dependent on impact locations and angles and the MCL is the most vulnerable ligament. Further, due to muscle effects, except when the impact is on the knee, peak strain values in all the ligaments are lower for an unaware pedestrian than either for a cadaver or for a fully braced pedestrian.

Keywords: Muscle Contraction, Hill Muscle Model, Pedestrian Safety, Knee Injury, Finite Element Modeling

THE ISSUE OF PEDESTRIAN SAFETY has been a matter of concern for public health practitioners and vehicle designers (Ashton et al., 1977). Pedestrians represent 65% of the 1.17 million people killed annually in road accidents worldwide (World Bank, 2001). Epidemiological studies on pedestrian victims have indicated that together with the head, the lower extremities are the most frequently injured body region (Chidester et al., 2001; Mizuno, 2003). The 2003 summary report of International Harmonized Research Activities (IHRA) Pedestrian Safety Working Group activity (Mizuno, 2003) has showed that 1,605 pedestrian victims in Australia, Germany, Japan and USA, sustained a total of 3,305 AIS 2+ injuries, out of which almost one third (32.6%) were to the lower extremity. To mitigate the incidences and extent of lower limb injuries, it is essential to understand the mechanism of these injuries.

Therefore, experiments using Post Mortem Human Specimen (PMHS) (Kajzer et al., 1990; 1993; 1997; 1999; Bhalla et al., 2005) have been conducted and injury mechanism has been studied. These experiments were intended to reproduce the loading environment of a pedestrian-car collision. For lack of better data, on the basis of results of these PMHS experiments FE models of the human body (Schuster et al., 2000; Maeno et al., 2001; Takahashi et al., 2001; Nagasaka et al., 2003; Chawla et al., 2004) have been validated.

Pedestrian Crash Data Study (PCDS) (Chidester et al., 2001) reports that passenger cars hold the major share in vehicle-pedestrian accidents and the front bumper is the major source of injury to lower extremity when injuries were caused by a vehicle structure (Mizuno et al., 2003). As the bumper height is low in passenger cars, it impacts a 50^{th} percentile male pedestrian at the knee or at locations just below the knee. The height of bumper varies with the type of a vehicle from passenger car, to minivan, to SUV's. Due to this the location of impact on lower extremity can also differ. Apart from this, it is reported that in real world, a pedestrian can be struck from various directions. Vehicle-pedestrian collision data shows that 57.5% impacts were from the lateral side, 30.3% from rear and

8.3% from the front. Forensic analysis of pedestrian collisions has demonstrated that the type of knee injury depends on the location and angle of impacts in relation to the knee joint (Teresinski et al., 2001).

Nagasaka et al. (2003) have investigated the knee injury process for various impact locations and angles using FE simulations and reported that knee injuries differ with impact locations and angles. However, the FE model used in their study did not include the effects of muscle contraction. In a preliminary investigation, Soni et al. (2006) reported that muscle activation decreases the probability of failure in knee ligaments in low speed lateral impacts. Recently, in Soni et al. (2007) a pedestrian lower limb FE model, called the Active Lower Extremity Model for pedestrian Safety (A-LEMS), including forty two lower extremity muscles and capable of simulating the failure in knee ligaments has been reported. The model was used to investigate the effects of muscular contraction on knee ligament failure for three different pre-impact conditions of a freely standing pedestrian in lateral impacts at below knee and ankle locations. The results of this study asserted that active muscle forces reduce the risk of ligaments failure and should be taken into account in predicting injuries in knee ligaments in pedestrian simulations.

This indicates that to devise effective pedestrian protection systems, it is important to assess if active muscle forces also affect knee injuries in pedestrians for various impact orientations. The current study extends the earlier study to investigate the effects of active muscle forces on failures in knee ligaments in lateral impacts at different impact locations and also varying impact angles. Simulations have been performed using the A-LEMS at five impact locations (ankle, mid tibia, below knee, on-knee and mid femur) and four angles (frontal, rear, 45 deg and 135 deg to anterior-posterior axis) at below knee level. Three sets of simulations, viz, 1. with deactivated muscles 2. with activated muscles (including reflex action) for an unaware pedestrian and 3. with muscles activated at full capacity (mimicking an aware pedestrian), have been performed for each impact orientation. Strains in knee ligaments and tibial displacements for different levels of muscle activation are then compared for each impact orientation to assess the effect of muscle forces.

DESCRIPTION OF A-LEMS

MODEL GEOMETRY AND VALIDATION STATUS

A-LEMS includes forty two muscles modeled as 1-D bar elements (Appendix A), in addition to the passive structures such as the cortical and the spongy parts of the femur, tibia, fibula, and the patella. The cortical part of the bones is modeled by shell elements while the spongy part is modeled by solid elements. Apart from these, passive muscle response and skin are also modeled using solid elements and membrane elements respectively. Knee ligaments, anterior cruciate ligament (ACL), posterior cruciate ligament (PCL), and lateral collateral ligament (LCL), have been modeled using solid elements. Because of a smaller thickness compared to width, the medial collateral ligament (MCL) has been modeled using the shell elements. The articular capsule i.e. “knee capsule”, which encloses the knee joint and maintains joint integrity, has also been included in this model. Additional details of geometric modeling of muscles are available in Soni et al. (2006 and 2007).

A-LEMS has been validated against available experimental data. Since all the available data is for cadaver tests, passive version of the A-LEMS was validated for different sets of loading and boundary conditions reported in Kajzer et al. (1997, 1999) and Kerrigan et al. (2003). These validation results have been presented in detail in Soni et al. (2007). The passive model validates for all the test conditions and can correctly reproduce impactor forces, knee kinematics and ligament failures reported from the experiments. Active muscles have then been incorporated in the passive model to develop A-LEMS.

HILL MODEL PARAMETERS

Muscle parameters, such as optimal muscle length (L_{opt}), maximum isometric force ($F_{\max}$), maximum contraction/ elongation velocity ($V_{\max}$), pennation angle (α), and an initial value of activation level (N_a), are used to define the Hill type muscle bar element. Values for the maximum

isometric force ($F_{\max}$), pennation angle (α) and the optimal muscle length (L_{opt}), at which a muscle produces maximum force; have been taken from Delp et al. (1990).

Maximum contraction velocity ($V_{\max}$) of a muscle depends upon the ratio of slow and fast type of fibers in it. A muscle containing more fraction of fast type of fibers can contract faster. Based on data available on mammalian muscles, Winters et al. (1985) has proposed an empirical relation (Eq. 1) between the maximum contraction velocity of a muscle and the fraction of fast type of fibers it contains.

$$V_{\max} = 2 * Lofib(s^{-1}) + 8 * Lofib(s^{-1}) * C_{fast} \qquad (1).$$

Where, L_{ofib} represents the muscle rest fiber length and C_{fast} fraction of fast fibers in a muscle.

Equation (1) has been used to calculate the maximum contraction velocity for each muscle and the data required for L_{ofib} and C_{fast} from Yamaguchi et al. (1990) have been used.

An activation level (N_a) represents the actuation state of a muscle. It is defined as the ratio of the applied force to the maximum force that can be exerted by a muscle. Thus it is a dimensionless quantity that ranges from a minimum value of 0.005 to maximum value of 1. An activation value of 0.005 represents a muscle at rest whereas maximum value (i.e.1) represents maximum activation in a muscle, such as that for maximum voluntary contraction (Winters et al., 1988). Data used to define the Hill muscle card of each muscle in A-LEMS has been listed in Appendix B

SIMULATIONS FOR STANDING POSTURE

SIMULATION SET UP

Fig. 1 shows the simulation set up used in present study. In all nine impact orientations have been simulated. In five orientations (named as ankle impact, mid tibia impact, below-knee impact, on-knee impact and mid femur impact) A-LEMS has been impacted at five different heights in the lateral direction. These locations have been selected to account for the variation of height of impact on pedestrian lower extremity due to the varying bumper height in different vehicles. In the remaining four orientations (named as frontal impact, 45 deg impact, 135 deg impact and rear impact), A-LEMS has been impacted at below knee level from different directions so as to study the effect of variation in the direction of impact.

In these simulations, A-LEMS has been configured as standing freely on rigid ground plate in a gravity field. Friction coefficient of 1.0 has been defined between the shoe and the ground in the simulations. A concentrated load of 250 N corresponding to half the body weight of a 50th percentile male (38.5 kg) minus weight of A-LEMS (13.95 kg) has been applied at the top of femur. A foam covered rigid impactor of 20 kg mass, propelled in the horizontal direction at a speed of 25 kmph to impact A-LEMS in various impact orientations as shown in Fig. 1. Bhalla et al. (2005) has reported that for a 50th percentile male, the centerline of the car bumper impacts the lower leg 45 mm below the tibia plateau. This value has been used to define the below knee level in our simulations.

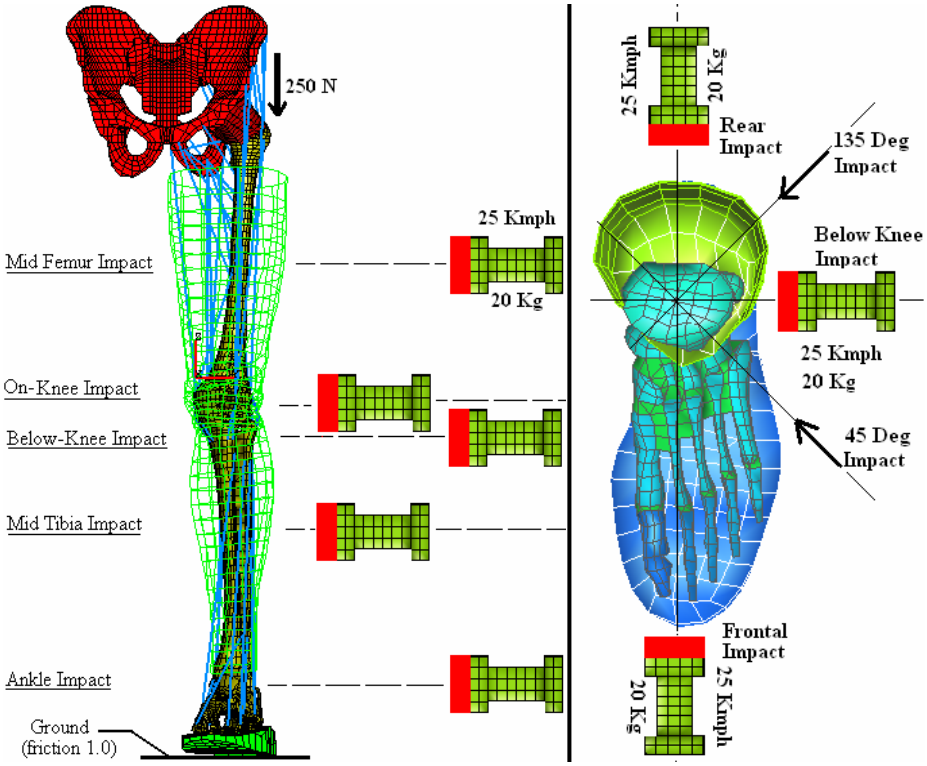

Fig. 1 – Simulation set up to study the effects of muscle forces in a freely standing pedestrian for five impact locations(left) and four impact angles at below knee level (right)

PEDESTRIAN PRE-IMPACT CONDITIONS

Three sets of simulations, viz, 1. with deactivated muscles 2. with activated muscles (including reflex action) for an unaware pedestrian and 3. with muscles activated at full capacity (mimicking an aware pedestrian, frozen in fright), have been performed for each impact orientation. In this paper these conditions have been named as cadaveric, reflex and braced (for fright) conditions respectively. These conditions differ in terms of initial activation levels in muscles and whether the reflex action is enabled. By enabling the reflex action for a muscle, the activation level in that muscle rises with time during the simulation which eventually increases the force produced by that muscle.

Cadaveric Condition: In this condition, a freely standing cadaver has been simulated. To model a cadaver in FE simulation, all the muscles in A-LEMS have been assigned the minimum value of 0.005 as an initial activation level. The reflex action is also kept disabled. Therefore, in this condition all the muscles function at their minimum capacity.

Reflex Condition: In this condition, a standing pedestrian who is unaware of an impending crash has been simulated. To model an unaware standing pedestrian in FE simulation, initial activation level required to maintain the stability of the standing posture of a pedestrian in gravity field (Kuo et al. (1993)) are assigned in the Hill material card of each muscle in A-LEMS. These activation values are listed in Table B1 in Appendix B.

A stretch based involuntary reflex action has also been enabled in this condition. For enabling the reflex, a threshold value of elongation is to be defined in Hill material card of a muscle. When the elongation in muscle crosses the threshold value, stretch reflex in a muscle gets activated. However, the increase in muscle force starts only after a certain time known as reflex time. This delay between the activation of stretch reflex and the onset of increase in muscle force represents the time taken by the signal to travel through the central nervous system (CNS) circuitry (muscle-spinal cord-muscle). A delay of 20 ms has been assigned to all the muscles in A-LEMS (Ackerman, (2002)). This mimics the ability of live muscle to respond to a small stretch produced by an outside agency. In medical terms this kind of reflex action is known as “stretch reflex”.

Braced Condition: In this condition a standing pedestrian, who is aware of an impending crash but is unable to escape from the site of collision and freezes in fright, has been simulated. To model this condition in simulation, bracing in all the muscles has been considered. It is assumed that a braced muscle functions at its maximum capacity. To simulate this condition, an initial activation level of 1 has been assigned to all the muscles. Reflex action is set off in this condition as all the muscles are already at their maximum activation level.

Two nodes at both femur and tibia have been selected to obtain the nodal time history in simulations. Locations of selected nodes are shown in Fig. 2. Relative movements of selected nodes are then used to calculate relative tibia displacements and knee joint angles. Fig. 2 shows the sign conventions used in the current study. Springs of very low stiffness are modeled on each knee ligament to calculate strain time history in simulations. However, element elimination approach has also been enabled to simulate the failure in knee ligaments. Response of cadaveric, reflex and braced conditions has been then compared to determine the role of muscle loading.

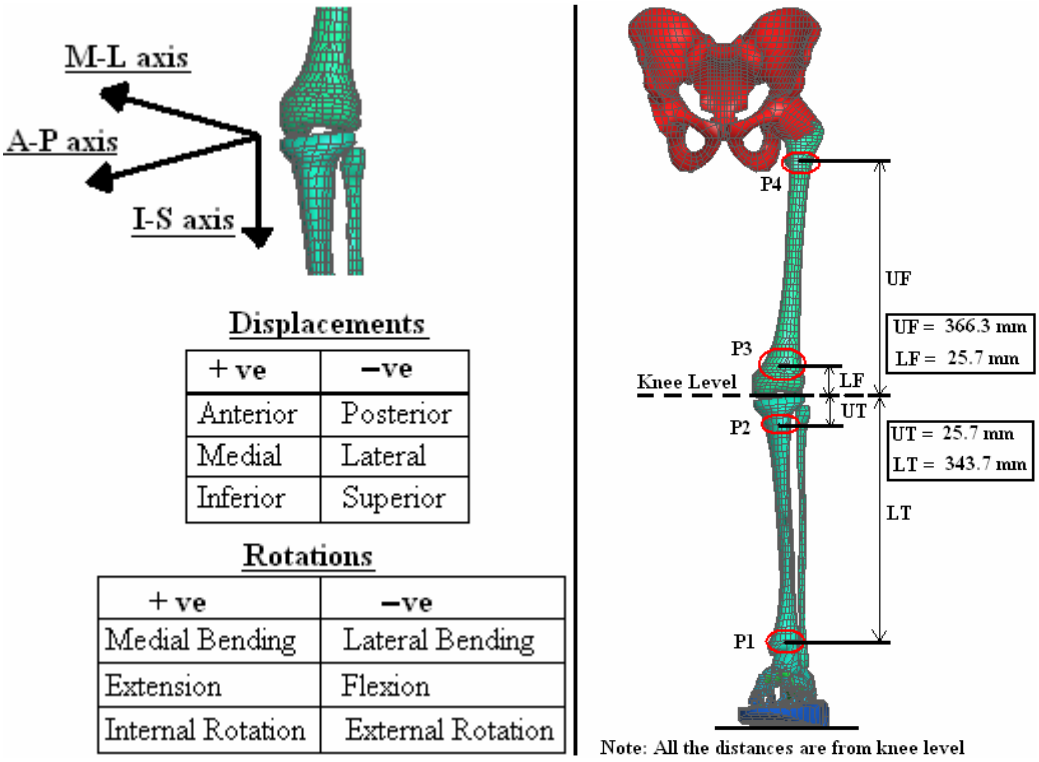

Fig. 2 – Sign conventions for relative tibia movements (left) and the locations of nodes at which nodal time histories have been obtained (right) in current study

RESULTS AND DISCUSSIONS

Before discussing the individual impact conditions, we discuss the kinematics and the loading as observed in these simulations.

It has been observed that for all the impact orientations, the impact response can be separated into two phases. In the initial phase (8-12 ms), the axially compressed lower extremity along with the friction at the foot resists the moving impactor. During this phase the impactor passes its kinetic energy in-elastically to the leg segments. Relative movement between tibia and femur starts only after the impactor force crosses a certain threshold. Relative tibia displacements at the knee joint level are observed to peak during this phase which leads to shear in the knee joint. We call this the impact phase.

In the second phase, which we call the inertial loading phase, the foot leaves the contact with the rigid ground and the lower leg comes into motion. Impactor force also starts diminishing. In this phase, the inertial effects have a dominating effect on knee kinematics. Relative angular displacements

between tibia and femur achieve peak values during this phase which result in further stretching the knee ligaments. As a result, ligament strains also attain peak values in this phase. However, ligament strains are dependent on the impact locations and orientations.

Relative tibia displacement in the initial phase of loading alters the position of the instantaneous center of rotations (CORs) of knee joint as well as relocates the attachment points of muscles on bones in space. Relocation of muscle attachment points modifies the direction of active muscle forces; however, change in position of the CORs varies the muscle moment arms. This causes change in direction and magnitude of the torques generated by the muscle forces. Consequently, these muscle forces and the generated torques no longer remain in equilibrium. The direction of the moment arm of a muscle relative to the modified CORs decides whether the muscle will support or resist the external load at knee joint. Thus active muscle forces alter the post impact kinematics of knee joint resulting in strain in knee ligaments. Stronger effects of muscle forces have been predicted in braced condition since muscles are functioning at their maximum capacity.

RESPONSE IN BELOW-KNEE IMPACT ORIENTATION

For each condition in below knee impact orientation, the impactor hits the lower leg laterally at just below the tibia plateau and compels it to translate in medial direction relative to femur for initial 5-8 ms. This induces strain in ACL and MCL. After 8 ms, in the inertial loading phase, knee joint kinematics changes from medial displacement to knee bending. Therefore, knee lateral bending angle starts increasing rapidly which eventually results in MCL failure. Rupture in MCL in below knee impact simulations agrees with the results of statistical analysis of real world accidents in which MCL is reported as the most frequently injured knee ligament (Matsui, 2001). By the time MCL fails, foot leaves the ground which frees the lower leg to move away from femur in inferior direction and eventually stretches the PCL. Even though active muscle forces alter the knee kinematics in braced and reflex conditions MCL continues to remain the most vulnerable ligament in the below knee impact.

Impact Force: Fig. 3.shows the impact force time history plots obtained in below knee impact orientation for each pre-impact condition (cadaveric, reflex, and braced) of a freely standing pedestrian. No significant differences have been observed in the impact force time history for all the three conditions. This is likely to be because the impact force direction is almost orthogonal to the direction of muscle forces and is hence not governed by the muscle activation but purely by the local dynamic interaction between the foam and the passive muscle.

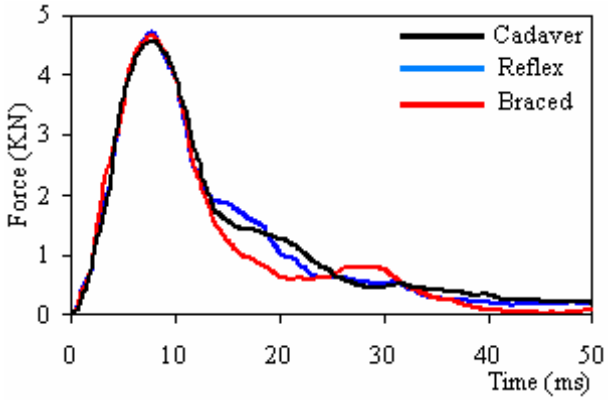

Fig. 3 – Comparison of impact force time history plots obtained in below knee impact orientation for three different conditions (cadaveric, reflex, and braced) of a freely standing pedestrian

It is observed that for each condition impactor force reaches its peak value of 4.55 KN about 8 ms after the initial contact with the leg. Till initial 5 ms of contact, no significant movement is noticeable at the knee joint. As the impactor force peaks, relative movement between tibia and femur has been observed. This event is the onset of ligament loading.

Knee Kinematics and Effect of Muscle Forces: Linear and angular displacements of tibia relative to femur are shown in Fig. 4 and Fig. 5 respectively. It is apparent that active muscle forces have significantly affected the knee joint kinematics in reflex and braced conditions as compared to cadaveric condition.

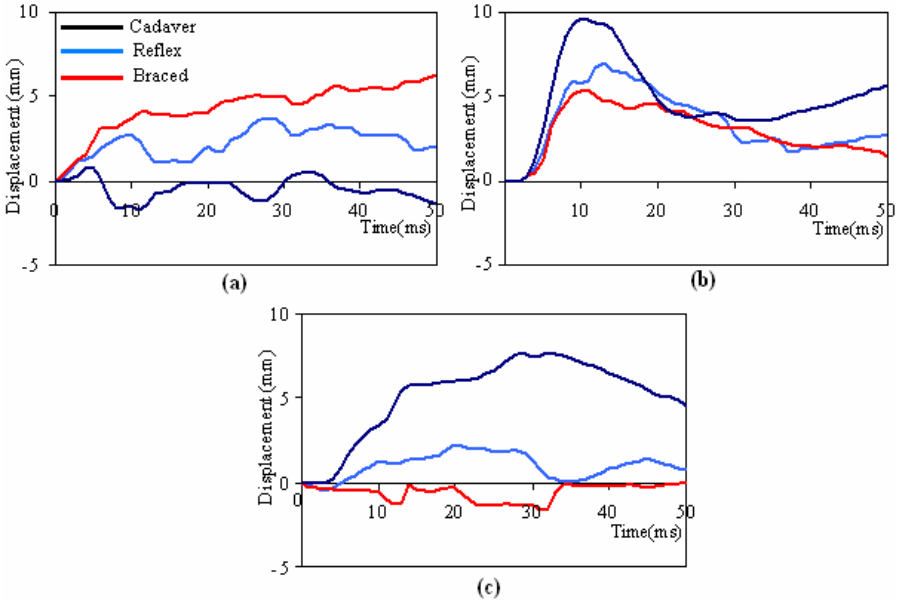

Fig. 4 – Comparison of relative tibia displacements (a) in anterior-posterior direction (b) in medial-lateral direction and (c) in inferior-superior direction obtained in below knee impact orientation for each condition (cadaveric, reflex, and braced) of a freely standing pedestrian

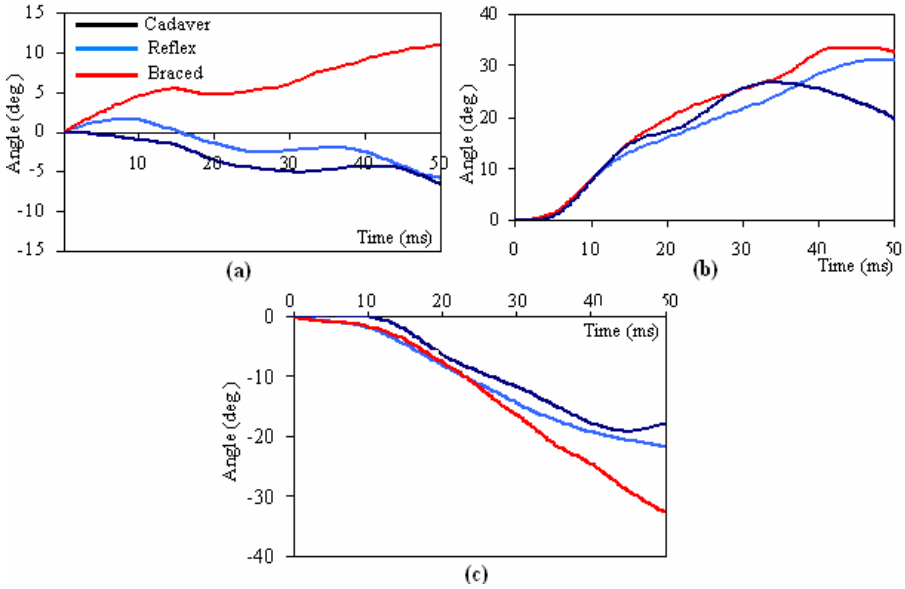

Fig. 5 - Comparison of relative knee angles (a) extension-flexion (b) medial-lateral bending and (c) internal-external rotation obtained in below knee impact orientation for each condition (cadaveric, reflex, and braced) of a freely standing pedestrian

Strain in Knee Ligaments and Effect of Muscle Forces: Fig. 6 illustrates the calculated strain time history in knee ligaments for each condition for below knee impact. It is evident that strain in knee ligaments is reduced significantly in the reflex and braced conditions as compared to the cadaveric condition.

ACL: Fig. 6 compares the strain time history in ACL for each condition. It is seen that strain in ACL remained lower for reflex and braced conditions as compared to cadaveric condition. Peak strain in ACL has dropped by a factor of 1.75 and 1.25 for reflex and braced conditions respectively.

Medial tibia displacement is the prime parameter which has induced strain in the ACL. Fig. 4 (b) compares the medial tibia displacement for each condition. It shows that due to muscle action, displacement of tibia has reduced for both reflex and braced conditions as compared to the cadaveric condition. This explains the reason of lower strain values in ACL. However, other parameters such as superior (or inferior) displacement of tibia (Fig. 4 (c)), which induces slacking (-ve) (or stretching (+ ve)) in ligaments also contribute to ACL strain.

Strain in ACL is found higher in braced condition than in the reflex condition. This could be due to the combined effect of increased anterior tibia displacement (Fig. 4 (a)) and knee extension (Fig. 5 (a)) for the braced condition.

PCL: Strain time history in PCL is compared for each condition in Fig. 6. It illustrates that strain in PCL is predicted to be lower under reflex and braced conditions as compared to the cadaveric condition. Peak strain in PCL has dropped by a factor of 3.85 for the reflex condition, however, reduction in peak strain value is even more pronounced (by 11 times) for the braced condition.

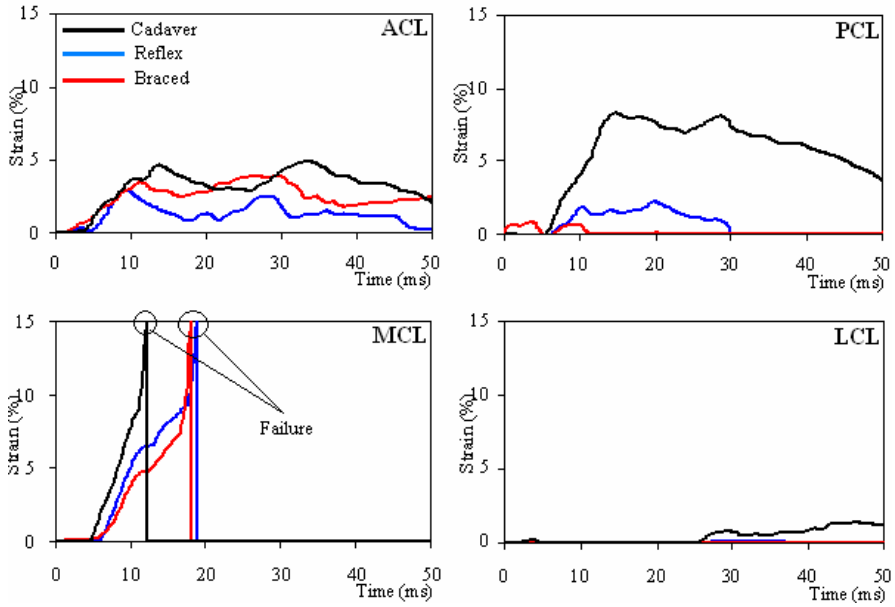

Fig. 6 - Comparison of strain in knee ligaments (ACL, PCL, MCL, and LCL) obtained in below knee impact orientation for each condition (cadaveric, reflex, and braced) of a freely standing pedestrian

Relative displacement of tibia in the inferior direction (Fig. 4 (c)) is the major source of strain in the PCL. Fig. 4 (c) depicts that in both the cadaveric and the reflex conditions, the tibia is moving away from the femur, thereby stretching the PCL. This displacement is higher for the cadaveric condition and therefore PCL strain is also higher in this condition. In case of the braced condition, Fig. 4 (c) shows negative tibial displacement which means that tibia is moving towards femur. This is because, as all the muscles are functioning at their full capacity, muscle forces are sufficiently high to pull the tibia towards the femur. This slackens the PCL.

MCL: MCL strain for each condition is shown in Fig. 6. It is observed that peak MCL strain reaches the ligament failure limit of 15% in each condition. However, in comparison to the cadaveric condition, failure is delayed by 6-7 ms in the other two conditions. Fig. 7 shows how rupture has occurred in the MCL in the simulations. Failure in all three conditions indicates that the energy of impact is sufficiently high to overpower the resistance provided by the muscle forces in the braced condition.

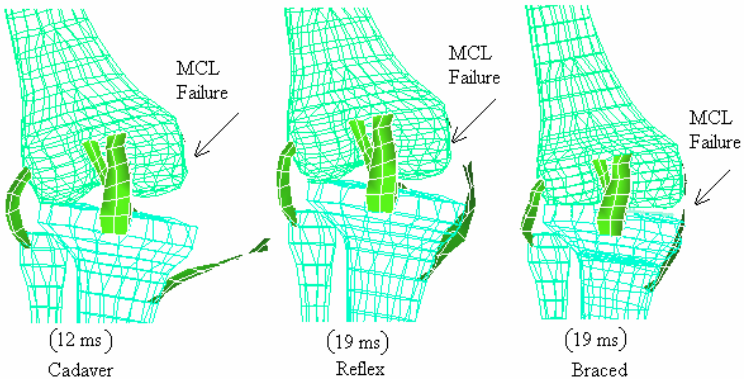

Fig. 7 – MCL failure in the below knee impact orientation for each pre-impact condition of a freely standing pedestrian

It is interesting to observe in Fig. 5 (b) that at 12 ms (which is the time of MCL failure in the cadaveric condition) the value of knee bending angle (10.6 deg) is identical for each condition. If the knee bending angle alone is considered as the prime parameter for MCL failure, then for each condition MCL should have failed at the same bending angle (10.6 deg) and at the same time (12ms). However, the time and the bending angles at failure (12ms / 10.6 deg in cadaveric, 19ms / 15.4 deg in the reflex and 19ms / 18.8 deg in the braced condition) are different in all the three conditions. From Fig. 4, it can be seen that at 12 ms (time of MCL failure in cadaveric condition), tibia displacement in medial (Fig. 4 (b)) and inferior (Fig. 4 (c)) directions are lower for reflex and braced conditions. This explains the reason of delay in MCL failure.

LCL: Fig. 6 illustrates that LCL strain is less than 1.5% in the cadaveric condition which has reduced to almost zero in the reflex and braced conditions. The low value of strain in LCL is ascribed to medial bending of the knee joint.

KINEMATICS FOR DIFFERENT IMPACT ORIENTATIONS

In this section we discuss the kinematics as observed in the simulations of the cadaveric condition under different impact configurations.

Variation in kinematics with impact height

The knee joint kinematics varies with the location of impact. We discuss the kinematics, in the five lateral impact configurations.

Ankle impact: In the ankle impact, the ankle is compelled to move medially relative to the knee joint. This initiates the rotation in tibia about its center of gravity (COG) and results in the lateral bending of the knee joint. Due to this, strain in LCL increases and reaches a peak value of 5.8% (at 15 ms). The foot leaves the ground at 10 ms, when the lateral knee bending has a peak value of 9 deg. Subsequently, due to inertial loads, the femur condyle starts slipping and rotating on the tibia plateau in the lateral direction. This continues till 40 ms after which knee bending changes from lateral to medial. This reduces the strain in LCL and increases the strain in the MCL to a peak value of 4% at 48 ms.

Mid Tibia Impact: In the mid tibia impact, the impactor hits the tibia at its COG. Therefore, in the initial loading phase medial tibia translation (10 mm at 15ms) is more prominent than tibia rotation (2.5 deg). This strains the ACL to about 2.7%. Subsequently, the foot also leaves the ground and the femur starts rotating laterally due to inertial loads. During 20 ms to 40 ms, medial tibia displacement and medial bending angle remain nearly constant (2.6 mm and 2.8 deg) as the lower extremity rotates about the hip joint. After 40 ms, a sudden rise in medial bending is observed, which results in rise in MCL strain (7.4% at 49 ms).

Below-Knee Impact: In the below-knee impact, tibia plateau moves in the medial direction. Therefore, in the initial phase of loading, medial tibia displacement reaches a peak value of 10 mm at 10 ms and the medial knee bending angle reached 8.5 deg. The MCL fails at 12 ms when the bending angle is 10.6 deg. The medial bending angle then increases rapidly as the resistance provided by the MCL has become zero. At 35 ms knee bending angle reaches a peak of 27 deg. Due to the large bending angle, a second peak in ACL time history is predicted (of 5% at 34 ms).

On-Knee Impact: In the on-knee impact orientation, the location of impact is such that it forces both tibia and femur to move in the medial direction. Therefore, a lower value of relative medial tibia displacement (less than 4 mm) is observed. However; high medial bending (28 deg) is observed as compared to other impact orientations. Failure in MCL has occurred at 9.4 ms when the bending angle is 9.83 deg.

Mid Femur Impact: In the mid femur impact, as the femur moves in the medial direction peak relative lateral tibia displacement of 6.75 mm is observed at 16 ms. This is accompanied by a medial bending of only about 1.85 deg, which increases to a peak value of 10.4 deg by 31 ms. At this point, LCL strain is a maximum at 6.5%. Subsequently, due to inertial loads, knee bending changes from medial to lateral at 39 ms. This relieves the strain in the MCL and causes strain in the LCL (7.5% at 49ms).

Variation in kinematics with impact angle

Knee joint kinematics also differs with the angle of impact. This is attributed to the movement of tibia plateau in the direction of impact.

Frontal Impact: In frontal impact, posterior tibia displacement (6mm at 15ms) and knee hyperextension (48.9 deg at 49 ms) is prominent. PCL and MCL failures are predicted at 18 and 42 ms respectively. PCL has failed due to the combined effect of posterior tibia displacement and knee hyperextension whereas; failure in MCL is ascribed to the knee hyperextension.

45 Deg Impact: In 45 deg impact, along with posterior tibia displacement (5 mm at 11 ms) and knee hyperextension (19 deg at 24 ms), medial tibia displacement (8.6 mm at 11 ms) and medial bending (18.5 deg at 35 ms) are also observed. This is because the impactor force has components in the anterior-posterior as well as medial-lateral directions. Failure is predicted in the PCL (at 25 ms) as well as in the MCL (at 27 ms). PCL fails due to the combined effect of posterior tibia displacement and knee hyperextension whereas; MCL fails due to the combined effects of medial displacement, medial knee bending and hyperextension.

135 Deg Impact: In 135 deg impact, along with anterior tibia displacement (7.6 mm at 13 ms) and knee flexion (26.3 deg at 32 ms), lateral tibia displacement (8.2 mm at 18 ms) and medial bending (13.7 deg at 22 ms) are also observed. This is because the impactor force has components in both anterior-posterior and medial-lateral directions. MCL failure is predicted at 13.5 ms when the medial bending is 9 deg. ACL strain of more than 5% is predicted due to the combined effect of anterior tibia displacement and medial bending.

Rear Impact: In rear impact, anterior tibia displacement (7.6 mm at 13 ms) and knee flexion (44.2 deg at 40 ms) are observed. This is ascribed to the forced tibia movement in the anterior direction. Strains in ACL, MCL and LCL are predicted to be more than 5%. ACL strain is due to the anterior tibia movement whereas; knee flexion causes strain in the MCL and LCL.

EFFECT OF MUSCLE FORCES FOR DIFFERENT IMPACT ORIENTATIONS

For all the impact orientations, ligament strains and the knee kinematics (linear and angular displacements) have been summarized and compared in this section.

Effect of Muscle Forces on ligament strains: Fig. 8 shows peak ligament strains in each condition for the various impact orientations.

Fig. 8 depicts that, for all impact orientations except the on-knee impact, peak ligament strain is lower in the reflex condition than that in the other conditions. Further, in the frontal and 45 deg impact

orientations reflex action in the muscles has even prevented the failure of MCL and PCL. This suggests that muscle reflex action (as compared to cadaveric condition) reduces ligament failure risk in eight out of the nine orientations.

However, for the braced condition ACL strain is higher for five impact orientations (ankle, mid tibia, mid femur, frontal and 45 deg impact) and PCL strain is higher for three impact orientations (ankle, mid tibia, mid femur impact). It is found that the bracing action in muscles has reduced the risk of LCL failure in all impact orientations and has prevented PCL from failing in the frontal and 45 deg impact orientations. Only in two impact orientations (on-knee and rear impact) muscle bracing has reduced the strain in all four ligaments. This shows that ligament failure risk is lower for the reflex condition as compared to braced condition for all the impact orientations except the on-knee and rear impacts.

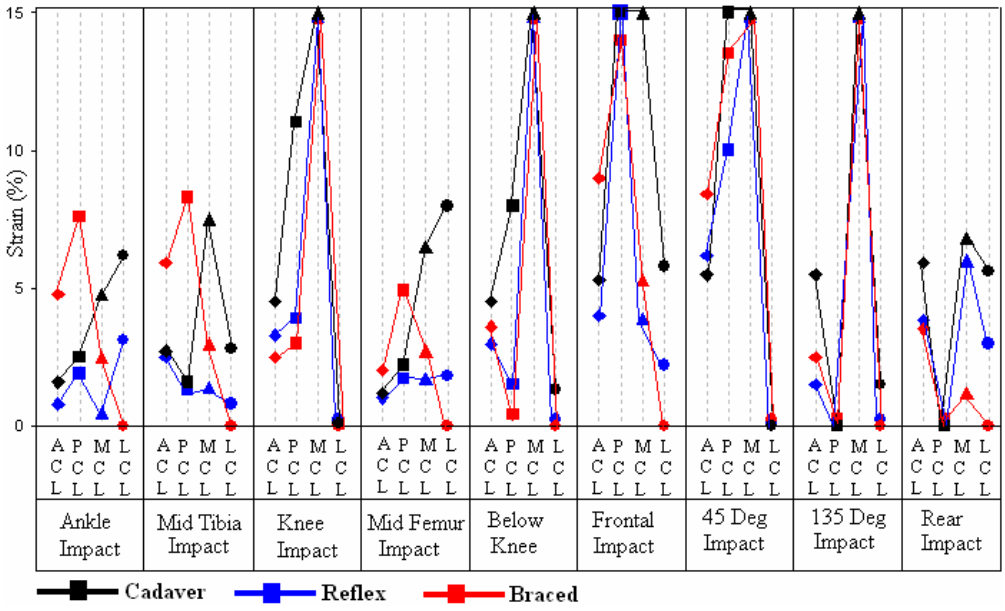

Fig. 8 – Comparison of peak strain value in knee ligaments (ACL, PCL, MCL, and LCL) calculated in various impact orientations for each condition (cadaveric, reflex, and braced) of a freely standing pedestrian

For each of the ligaments, we now discuss the difference in the reflex and the braced behavior in these impact orientations.

ACL: Peak ACL strain is higher for the braced condition in five impact orientations (ankle, mid tibia, mid femur, frontal and 45 deg impact). The potential parameters causing ACL strain are shown in Table 1

Table 1 Factors affecting ACL strain in different impact orientations

Impact Orientation	**Factors causing increased ACL strain in the braced condition**
Ankle and Mid tibia impact	higher anterior tibia displacement
mid femur impact	higher internal tibia rotation
frontal impact	combined effects of anterior displacement, medial tibia displacement and knee hyperextension
45 deg impact	combined effects of anterior displacement and hyperextension

PCL: Peak PCL strain is higher for the braced condition in ankle, mid tibia and mid femur impacts. This is due to the knee extension in ankle and mid tibia impacts and negative displacement (lateral) of tibia relative to femur in mid femur impact.

MCL: Peak MCL strain is higher for the braced condition as compared to the reflex condition in four impact orientations. This could be due to lower negative bending (lateral) angle in ankle impact, higher medial bending angle in mid tibia and mid femur impact, and higher medial displacement in frontal impact.

LCL: Peak LCL strain is lower for the braced condition as compared to the other conditions in all impact orientations. This is likely to be because of tibial displacement in the superior direction.

Effect of Muscle Forces on Knee Kinematics: Fig. 9 shows the peak values of relative knee displacements calculated in each condition for impact at different locations and angles.

In Fig. 9(a) posterior tibial displacement has been observed in frontal and 45 deg impact orientations (C6 and C7) for cadaveric and reflex conditions. This is attributed to the forced movement of tibia plateau in posterior direction.

In all the impact orientations, superior tibia displacement is observed for the braced condition (Fig. 9(c)). This could be explained as for the braced condition all the muscles are functioning at their full capacity and the active muscle forces are sufficiently high to pull the tibia towards femur.

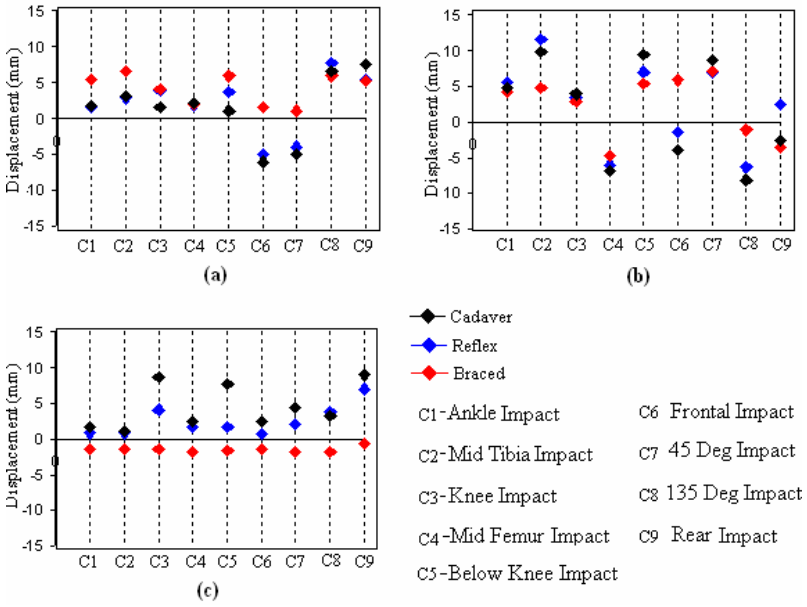

Fig. 9 - Comparison of peak value of relative tibia displacements (a) in anterior-posterior direction (b) in medial-lateral direction and (c) in inferior-superior direction calculated in various impact orientations for each condition (cadaveric, reflex, and braced) of a freely standing pedestrian

Fig. 10(a) shows higher values of knee extension (hyperextension) for the frontal and 45 deg impact orientations (C6 and C7). In contrast, higher knee flexion angle is noticeable for 135 deg as well as rear impacts (C8 and C9). This is ascribed to the direction of impact.

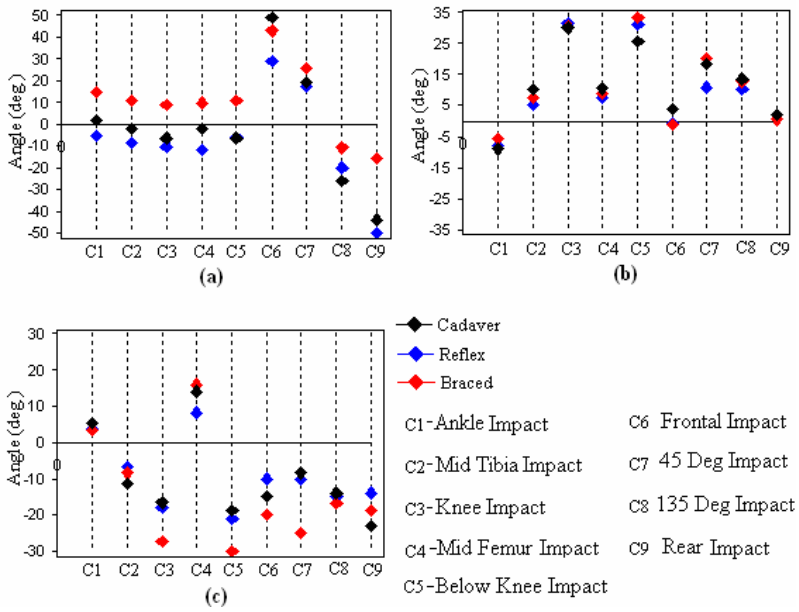

Fig. 10 - Comparison of peak value of relative knee angles (a) extension-flexion (b) medial-lateral bending and (c) internal-external rotation calculated in various impact orientations for each condition (cadaveric, reflex, and braced) of a freely standing pedestrian

CONCLUSIONS

A-LEMS has been used to investigate the effects of active muscle forces on knee ligament loading and failure under impact. Lateral impacts at five locations (ankle, mid tibia, below knee, on-knee and mid femur) and four angles (frontal, rear, 45 deg and 135 deg to anterior-posterior axis) at below knee level have been studied. Differences in response between a cadaver, an unaware pedestrian (with active muscles) and a (aware) braced pedestrian (frozen in fright), have been studied. To assess the effect of muscle activation, strains in knee ligaments and knee joint kinematics have been compared in each impact orientation. Results of the present study indicate that the active muscle forces significantly affect the loading at the knee ligaments. Therefore muscle activation should be taken into account while devising the pedestrian safety regulations. Finally following conclusions can be drawn.

1. Knee ligament strains depend on impact locations and angles. For the nine impact orientations studied MCL is predicted to rupture in five orientations (on-knee, below knee, frontal, 45 deg and 135 deg impact). The PCL is predicted to rupture in two orientations (frontal impact and 45 deg impact) Therefore, MCL could be considered to be the most vulnerable ligament followed by the PCL.
2. Muscle forces alter knee joint kinematics and consequently alter knee ligament loads.
3. In the reflex condition peak ligament strains were lower than those in other conditions, except in the on-knee impact condition. Therefore, the risk of ligament failure in real life crashes is likely to be lower than that predicted through cadaver tests / simulations.
4. Compared to the reflex condition, for the braced condition, peak ACL strain was higher in five orientations while the peak LCL strain is lower in all the orientations. This implies that in case of a crash, ACL could be at higher risk whereas LCL could be saved if the pedestrian braces himself.

LIMITATIONS AND FUTHER IMPROVEMENTS

In A-LEMS, we have adopted a straight line geometric model of the muscle because of the simplicity of definition using the origin and insertion locations of a muscle. This approach can lead to errors for muscles which do not work in a straight line (gracilis, semitendinosis, tibialis posterior, flexor digitorium longus, flexor hallucis longus, tibialis anterior, extensor hallucis longus, extensor digitorium longus, peroneus tertius, peroneous brevis, and peroneus longus). Multiple points could be used in the muscle definition to account for the curved path of some muscles.

For further improvements in the current finite element model, tendons should also be modeled along with the muscles to consider their effects. Present model considers only the upper body mass; however the inclusion of its detailed geometry may affect the kinematics of knee joint. The study also needs to be extended to other impact configurations as well as muscle conditions.

References

1. Ackerman, U., PDQ Physiology 2002, www.fleshandbones.com/readingroom/pdf/226.pdf
2. Bhalla, K., Takahashi, Y., Shin, J., Kam, C., Murphy, D., Drinkwater, C., and Crandall, J., Experimental investigation of the response of the human lower limb to the pedestrian impact loading environment, In Proceedings of the Society of Automotive Engineer World Congress 2005, SAE Paper 2005-01-1877.
3. Chawla, A., Mukherjee, S., Mohan, D., and Parihar, A., Validation of lower extremity model in THUMS, In Proceedings of the IRCOBI 2004, pp. 155-166.
4. Delp, S. L., Loan, J. P., Hoy, M. G., Zajac, F. E., Topp, E. L., Rosen, J. M., An interactive graphics-based model of the lower extremity to study orthopaedic surgical procedures, IEEE Trans. Biomed. Eng. 1990, Vol. 37, pp. 757-767.
5. Chidester, A. B., and Isenberg, R. A., Final report - the pedestrian crash data study, In Proceedings of the 17th ESV conference 2001.
6. Kajzer, J., Cavallero, S., Ghanouchi, S., and Bonnoit, J., Response of the knee joint in lateral impact: Effect of Shearing Loads, In Proceedings of the IRCOBI 1990, pp. 293-304.
7. Kajzer, J., Cavallero, S., Bonnoit, J., Morjane, A., and Ghanouchi, S., Response of the knee joint in lateral impact: Effect of Bending Moment, In Proceedings of the IRCOBI 1993.
8. Kajzer, J., Schroeder, G., Ishikawa, H., Matsui, Y., and Bosch, U., Shearing and bending effects at the knee joint at high speed lateral loading, In Proceedings of the Society of Automotive Engineers 1997, SAE Paper 973326.
9. Kajzer, J., Ishikawa H., Matsui Y., and Schroeder G., Shearing and bending effects at the knee joint at low speed lateral loading, In Proceedings of the Society of Automotive Engineers 1999, SAE Paper 1999-01-0712.
10. Kuo, A. D., and Zajac, F. E., A biomechanical analysis of muscle strength as a limiting factor in standing posture, Journal of Biomechanics 1993, Vol. 26, pp. 137-150.
11. Maeno**,** T., and Hasegawa, J., Development of a finite element model of the total human model for safety (THUMS) and application to car-pedestrian impacts, In Proceedings of the 17th ESV conference 2001, Paper No. 494.
12. Mizuno**,** Y., Summary of IHRA Pedestrian safety WG activities (2003) – proposed test methods to evaluate pedestrian protection afforded by passenger cars, In Proceedings of the 18th ESV conference 2003.
13. Nagasaka, K., Mizuno, K., Tanaka, E., Yamamoto, S., Iwamoto, M., Miki, K,. and Kajzer J., Finite element analysis of knee injury in car-to-pedestrian impacts, Traffic Injury Prevention 2003, Vol. 4, pp. 345-354.
14. Schuster, J. P., Chou, C. C., Prasad, P., and Jayaraman, G., Development and validation of a pedestrian lower limb non-linear 3-D finite element model, Stapp Car Crash Journal 2000, Paper No. 2000-01-SC21.
15. Soni, A., Chawla, A., and Mukherjee, S., Effect of muscle active forces on the response of knee joint at low speed lateral impacts, In Proceedings of the Society of Automotive Engineers World Congress 2006, SAE Paper 2006-01-0460.
16. Soni, A., Chawla, A., and Mukherjee, S., Effect of muscle contraction on knee loading for a standing pedestrian in lateral impacts, Accepted in 20th ESV conference 2007, Paper No. 467.
17. Tresinski, G., and Madro, R., Knee joint injury as a reconstructive factor in car-pedestrian accidents, Forensic Science International 2001, Vol. 124, pp. 74-82.
18. Takahashi, Y., and Kikuchi, Y., Biofidelity of test devices and validity of injury criteria for evaluating knee injuries to pedestrians, In Proceedings of the 17th ESV conference 2001.
19. World Bank Road Safety 2001, http://www.worldbank.org/transport/roads/safety.html
20. Yamaguchi, G., Sawa, A., Moran, D., Fessler, M., and Winters, J., A survey of human musculotendon actuator parameters. In: Winters, J., and Woo, S., (Eds.) Multiple Muscle Systems, Springer, New York 1990, pp. 717-773.

ACKNOWELEDEGEMENT

The authors would like to acknowledge the support from the Transportation Research and Injury Prevention Program (TRIPP) at Indian Institute of Technology Delhi and the Volvo Research Foundation. The authors also acknowledge Toyota Central Research and Development Lab (TCRDL) for providing the finite element human body model, Total Human body Model for Safety (THUMS) which was used in an earlier version of this study.

APPENDIX – A

Muscles of the lower extremity modeled

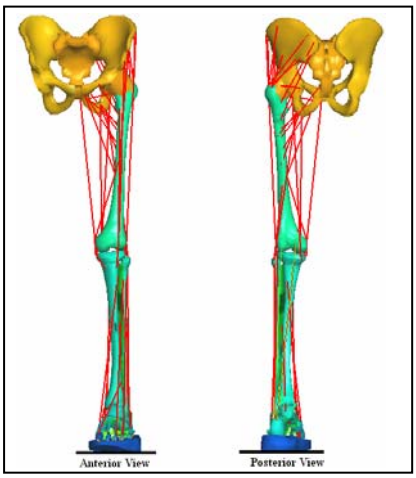

Fig. A1 - Anterior (left) and Posterior (right) views of A-LEMS showing 42 lower extremity muscles modeled as 1-D bar elements for the standing posture of a pedestrian

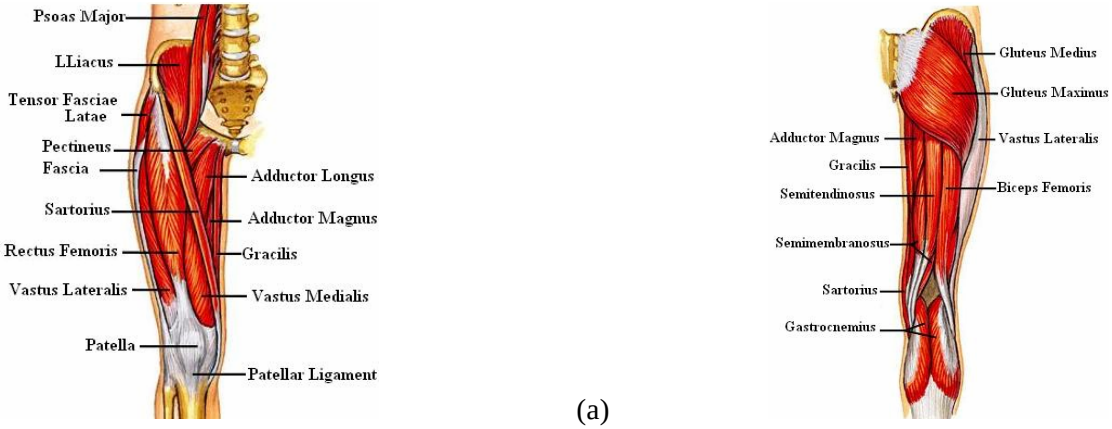

(a)

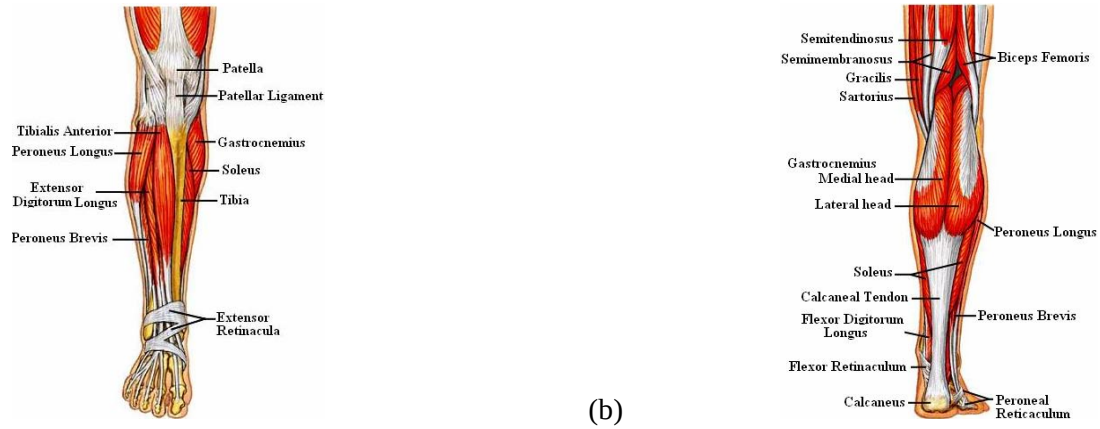

(b)

Fig. A2 – Anterior (right) and posterior (left) views of human (a) thigh and (b) lower leg muscles.

APPENDIX – B

Muscle parameters used

Forty two lower extremity muscles are defined in the local reference frames according to White et al. (1989). Data used to define Hill muscle card for a muscle are listed below in Table B.1.

Table B.1: Muscle data used

Lower extremity muscles	F_{max} (N)	L_{opt} (m)	C_{fast}	aV_{max} (V_{max} / L_{opt})	N_a
Vastus Lateralis	1871	0.084	0.52	5.85	0.005
Vastus Intermedius	1365	0.087	0.5	5.10	0.005
Vastus Medialis	1294	0.089	0.53	5.36	0.005
Rectus Femoris	779	0.084	0.619	5.55	0.005
Soleus	2839	0.03	0.25	2.67	1*
Gastrocnemius Medialis	1113	0.045	0.518	5.74	1*
Gastrocnemius Lateralis	488	0.064	0.518	5.69	1*
Flexor Hallucis Longus	322	0.043	0.5	5.17	0.005
Flexor Digitorium Longus	310	0.034	0.5	4.58	0.005
Tibialis Posterior	1270	0.031	0.5	4.65	1*
Tibialis Anterior	603	0.098	0.27	3.28	0.5*
Extensor Digitorium Longus	341	0.102	0.527	5.31	0.005
Extensor Hallucis Longus	108	0.111	0.5	4.32	0.005
Peroneus Brevis	348	0.05	0.375	4.59	1*
Peroneus longus	754	0.049	0.375	4.35	0.005
Peroneus Tertius	90	0.079	0.375	4.76	0.005
Biceps Femoris (LH)	717	0.109	0.331	3.55	1*
Biceps Femoris (SH)	402	0.173	0.331	3.91	1*
Semimembranosus	1030	0.08	0.5	5.61	1*
Semitendinosus	328	0.201	0.5	4.76	1*
Piriformis	296	0.026	0.5	5.71	0.005
Pectineus	177	0.133	0.5	4.62	0.005
Obturatorius Internus	254	0.049	0.5	5.71	0.005
Obturatorius Externus	109	0.030	0.5	5.71	0.005
Gracilis	108	0.352	0.5	5.13	0.005
Adductor Brevis 1	286	0.133	0.5	5.17	0.005
Adductor brevis 2	286	0.133	0.5	5.22	0.005
Adductor Longus	418	0.138	0.5	4.69	0.5*
Adductor Mangus 1	346	0.087	0.416	5.07	0.005
Adductor Mangus 2	444	0.121	0.416	5.07	0.005
Adductor Mangus 3	155	0.131	0.416	5.07	0.005
Gluteus Maximus 1	382	0.142	0.476	5.53	0.005
Gluteus Maximus 2	546	0.147	0.476	5.53	0.005
Gluteus Maximus 3	368	0.144	0.476	5.53	0.005
Gluteus Medius 1	546	0.054	0.5	5.71	0.005
Gluteus Medius 2	382	0.084	0.5	5.71	0.005
Gluteus Medius 3	435	0.065	0.5	5.71	0.005
Gluteus Minimus 1	180	0.068	0.5	5.71	0.005
Gluteus Minimus 2	190	0.056	0.5	5.71	0.005

Gluteus Minimus 3	215	0.038	0.5	5.71	0.005
Sartorius	104	0.579	0.504	5.03	0.005
Tensor Fasciae Latae	155	0.095	0.5	5.71	1*

* These values of muscle activation levels have been taken from Kuo et al. (1993)

Back